Stabilization of the amorphous state of pharmaceuticals in nanopores†

G. T. Rengarajan,[a] D. Enke,[b] M. Steinhart[c] and M. Beiner*[a]

Received 12th March 2008, Accepted 16th April 2008
First published as an Advance Article on the web 30th April 2008
DOI: 10.1039/b804266g

Confinement in nanoporous host systems with strongly interacting pore walls is shown to be a powerful approach to increase the lifetime of amorphous drugs based on changes in thermodynamics and crystallization kinetics in nano-sized systems.

Amorphous drugs are an interesting class of substances for pharmaceutical applications.[1] Their main advantage as compared to conventional crystalline drugs is their considerably improved solubility and bioavailability.[2] For real-life applications the production of amorphous drugs persisting for long periods of time under common storage conditions is indispensable. Unfortunately, many amorphous pharmaceuticals show a strong tendency towards crystallization that cannot be suppressed completely during typical shelf times. As a result, it is difficult or even impossible to achieve controllable drug release. Here we show that confining drugs to nanoporous host systems with strongly interacting pore walls allows this problem to be overcome and that long-term stable amorphous drugs can be produced.

At least three effects can lead to significantly increased lifetimes of amorphous drugs in nanoporous host systems. (i) Equilibrium thermodynamics predicts that crystallization is completely suppressed below a certain critical pore diameter d^* since surface energy contributions overcompensate the energetic advantage associated with the release of internal energy upon crystallization. In the case of cylindrically shaped pores the critical diameter can be estimated from[3]

$$d^* = 4\sigma_{cl}T_m^{\infty}/[(T_m^{\infty} - T)\Delta H_m\rho_c] \quad (1)$$

with σ_{cl} being the surface energy between crystal and melt, ΔH_m the heat of melting, T_m^{∞} the bulk melting temperature and ρ_c the crystal density. Typically, d^* amounts to a few nanometers.[3] (ii) Changes in the nucleation mechanism may delay the crystallization if a liquid is confined in isolated nanopores since each compartment must be nucleated independently.[4] Homogeneous nucleation will dominate under these conditions as long as the pore walls are non-nucleating. This leads to longer crystallization times τ_c in the case of isothermal crystallization or lower crystallization temperatures in non-isothermal crystallization experiments. (iii) The crystallization kinetics can slow significantly in nanopores since immobilized surface layers having a thickness of about one nanometer may form on pore walls with high surface energy.[5] This effect will be most relevant in very small nanopores where the fraction of interfacial material is huge and in cases where strong hydrogen bonds are formed at the interface. While the first phenomenon (i) is a thermodynamic equilibrium effect the other two (ii,iii) change the crystallization kinetics.

DSC experiments performed on a series of controlled porous glasses (CPGs) filled with acetaminophen (ACE, $C_8H_9NO_2$, inset Fig. 1a), which is an analgesic and anti-pyretic drug occurring in three different crystalline forms,[6] show clearly that nanoconfinement can indeed be exploited to stabilize the amorphous state of drugs. CPGs are nanoporous host systems with well-defined pore diameter, large porosity and sponge-like topology (*cf.* ESI†). The untreated pore walls are hydroxyl-terminated and able to form hydrogen bonds with guest molecules. 300 μm thick CPG membranes were infiltrated by immersing them in molten ACE heated to 180 °C. Crystallization of the material confined to the pores occurs at first in the presence of a macroscopic ACE surface layer during cooling. Subsequently, the surface layer was carefully removed with a scalpel and small pieces of the samples (~10 mg) were encapsulated in hermetically sealed DSC pans. In the case of bulk ACE (Fig. 1a) crystallization can be avoided by melt quenching with cooling rates faster than −100 K min^{-1} but crystallization occurs afterwards either during reheating, as indicated by a cold crystallization peak between 80 and 100 °C (2nd heating), under isothermal conditions at 80 °C within minutes (3rd heating), or at room temperature on a time scale of a few days.[7,8] The orthorhombic crystalline form II of ACE, which melts near 157 °C, is found in all these cases instead of the monoclinic form I which is the most stable and commercially used crystalline form that melts at 167–169 °C.[6] If ACE is confined to CPGs having pores with average diameters between 20 and 100 nm and untreated pore walls, the crystallization behaviour changes. The results obtained for ACE confined to 43 nm pores are shown in Fig. 1b as an example. Melting of form I is observed in the 1st heating scan, performed on as-prepared samples that were completely crystallized during initial cooling in the presence of a thick ACE surface layer. The melting peak of form I appears in this case at 161 °C in accordance with the melting point depression predicted by the Gibbs–Thomson plot shown in the inset of Fig. 1c. Based on porosity P (ESI,† Table SI) and heat of melting of form I ($\Delta H_{m,I}$ =186.1 J g^{-1}), it can be concluded that our CPGs are nearly completely filled and that the crystallinity of ACE is close to 100%. In the 2nd heating scan, performed after quenching the sample without macroscopic ACE surface layer in the DSC with a nominal rate[9] of −200 K min^{-1} from 180 °C to −40 °C, a glass transition near 24 °C (inset Fig. 1b) and a cold crystallization peak above 80 °C are observed like in the bulk. The main difference compared to the bulk sample is that the conventionally inaccessible form III of ACE[10] is found, which melts at around 136 °C in CPGs with d = 43 nm. The appearance of

[a]*Institut für Physik, Martin-Luther-Universität Halle-Wittenberg, 06099 Halle (Saale), Germany; Fax: +49-345-5527351; Tel: +49-345-5525350*
[b]*Institut für Chemie, Martin-Luther-Universität Halle-Wittenberg, 06099 Halle (Saale), Germany*
[c]*Max-Planck Institut für Mikrostrukturphysik, Weinberg 2, 06120 Halle (Saale), Germany*

† Electronic supplementary information (ESI) available: Details about materials, sample preparation, instruments and additional WAXS and DSC data. See DOI: 10.1039/b804266g

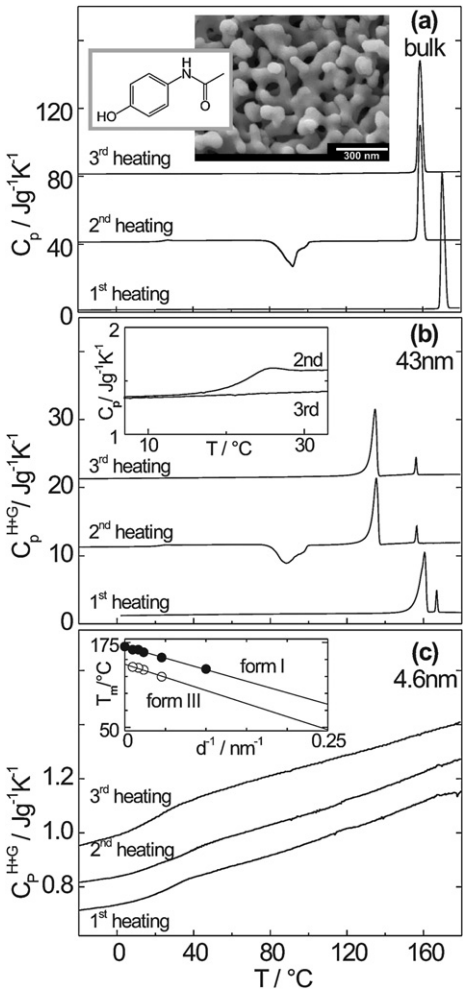

Fig. 1 DSC heating scans ($dT/dt = 10$ K min^{-1}) for ACE in (a) the bulk state or confined in CPGs with pore diameters of (b) 43 nm and (c) 4.6 nm after different thermal treatments. Three heating scans are shown in each individual plot. The 1st heating scan is measured on (a) as-received ACE or (b,c) infiltrated CPGs quenched while covered with a bulk ACE surface film and measured after the removal of the ACE surface films. The 2nd heating scan is measured after quenching the samples from 180 °C to −40 °C at a nominal rate of −200 K min^{-1}.[9] The 3rd heating is measured after DSC quenching (−200 K min^{-1}) and isothermal crystallization (a) at 80 °C for 12 min, (b) at 80 °C for 120 min, or (c) at 35 °C for 120 min. The curves are vertically shifted by (a) 40 J g^{-1} K^{-1}, (b) 10 J g^{-1} K^{-1} or (c) 0.1 J g^{-1} K^{-1}. The heat capacity of the host–guest system is plotted in (b,c). Small fractions of surface material melt in the case of the CPG with 43 nm pores at around $T_{m,I} = 167$ °C (1st heating) or $T_{m,II} = 156$ °C (2nd and 3rd heating).[7a] Insets: (a) scanning electron microscopy image of a CPG and chemical structure of ACE. (b) Thermal glass transition of ACE in 43 nm pores. (c) Melting temperature T_m *vs.* inverse pore diameter $1/d$ of form I and form III of ACE. The lines are fits to the Gibbs–Thomson equation for cylindrical crystals $T_m^\infty - T_m(d) = 4\sigma_{cl}T_m^\infty/[d\Delta H_m\rho_c] = s/d$ with $T_{m,III}^\infty = 143$ °C and $s_{III} = 386$ K nm for form III and $T_{m,III}^\infty = 169$ °C and $s_{III} = 340$ K nm for form I.

form III under these conditions has been also confirmed by wide angle X-ray scattering experiments (*cf.* ref. 7*a*; ESI,† Fig. S1). The behaviour shown in Fig. 1b is common for ACE in CPGs with pore diameters of 20 nm < d < 100 nm[7a] and only a shift of the melting peaks along with decreasing d values according to the Gibbs–Thomson equation occurs (inset Fig. 1c). Note that form III of acetaminophen is also found in porous alumina with similar pore diameters,[7a] another host system where hydrogen bonds can be formed at the pore walls, and that the appearance of unstable crystalline forms in nanoporous host systems has been reported recently also for other polymorphic materials and drugs.[11]

Qualitative changes are seen in the DSC scans for ACE in CPGs with an average pore diameter d significantly smaller than 10 nm. The heating scans for ACE in 4.6 nm pores are shown in Fig. 1c. A broad glass transition between 10 and 40 °C is observed in the 1st and in the 2nd heating scan, whereas melting peaks and exothermal cold crystallization peaks are completely absent. The 3rd scan evidences that no isothermal crystallization occurs during annealing at 35 °C. Melting peaks are neither seen after annealing for 120 min (Fig. 1c) nor after annealing for several weeks at this temperature (ESI,† Fig. S2). We used $T_c = 35$ °C here since the melting temperature of form III crystals in 4.6 nm pores should be $T_{m,III}(4.6\text{ nm}) = 50$–$60$ °C according to an extrapolation based on the Gibbs–Thomson equation (inset Fig. 1c). This is far below 80 °C where rapid cold crystallization occurs in bulk ACE. Obviously, the confined drug remains completely amorphous for very long times at all crystallization temperatures $T_g < T_c < T_{m,III}(4.6\text{ nm})$. Note that crystallization experiments performed above the melting temperature of form III do not lead to crystallization, as expected. Fast crystallization significantly below T_g seems to be unlikely also. Thus, crystallization of ACE appears to be completely suppressed in CPGs with 4.6 nm pores. Based on information about the sample mass before and after filling with ACE, solubility tests and estimated Δc_p values at the ACE glass transition we conclude that the degree of filling in case of CPGs with 4.6 nm pores is at least 70%.

The glass transition of ACE in the 4.6 nm pores around 20 °C is significantly broader as compared to that in the larger pores and in the bulk. This indicates that the confined drug has a spatially inhomogeneous mobility and density. Similar behaviour was reported for several liquids which are able to form hydrogen bonds like water,[5d] salol and glycerol[5a] confined to nanoporous host systems and attributed to the presence of immobilized surface layers with a thickness of 0.4–1 nm. In this connection, two separated glass transitions are often observed. We have also occasionally found indications of two distinct glass transitions (ESI,† Fig. S3) for ACE confined to nanoporous Vycor glass with an average pore diameter of 4 nm (Vycor Brand Porous Glass 7930 by Corning Inc.). Apparently, the packing of amorphous ACE in the pores depends sensitively on the properties of the nanoporous host system and on the conditions under which the samples were prepared. The complete suppression of the crystallization of ACE in CPGs with 4.6 nm pores was confirmed by the experiments carried out with nanoporous Vycor glass.

The persistence of amorphous ACE under nanoconfinement can be explained thermodynamically if the critical diameter d^* of the nuclei for the crystalline form III is larger than the pore diameter d. Using eqn (1) and the slope of the curve in the Gibbs–Thomson plot (inset Fig. 1c), $s_{III} = 4\sigma_{cl}T_m^\infty/[\Delta H_m \cdot \rho_c] = 386$ K nm, one can estimate $d^*(35\text{ °C}) \sim 3.6$ nm.[12] Under conditions where $d^* > d$ the nuclei cannot reach the size necessary for exergonic crystal growth. Hence, the amorphous state would be thermodynamically stable.[3] ACE confined to 4.6 nm pores is very close to this limit and consistently crystalline ACE could not be found in that case. However, an alternative explanation for this finding is based on the assumption that the crystallization kinetics at 35 °C is strongly slowed compared

to bulk ACE.[8] Since form III crystals in 4.6 nm pores should melt at 50–60 °C, any crystallization temperature at which form III crystals can grow must be significantly lower than the conventional cold crystallization temperatures of bulk ACE ($T_c \sim 80$ °C). The mobility at these temperatures might be too small to observe crystallization on an accessible time scale. A reduced number of heterogeneous nuclei fitting to extremely small pores could also contribute to a slower kinetics. A transition from heterogeneous to homogeneous nucleation, however, seems to be unlikely since there are no isolated subvolumes in CPGs that have sponge-like topology and interconnected pores. At the moment, it is not trivial to elucidate whether or not amorphous ACE is the equilibrium state in 4.6 nm pores. If the kinetics is extremely slow, crystallization might occur only on time scales which are not accessible experimentally. For the use of confined amorphous drugs in real-life applications, however, this fundamental question might be less important since the major criterion is here that the amorphous state is stable under typical storage conditions for a specific shelf time.

The presented results for an ACE/CPG model system demonstrate nicely that the discussed approach to prevent crystallization by nanoconfinement is applicable to amorphous drugs. Criteria that should be fulfilled by other suitable host systems can be derived. As described above, there are thermodynamic as well as kinetic effects, which can be exploited to increase the lifetime of the amorphous state. If the pores are sufficiently small ($d < d^*$) crystallization will never occur since the amorphous drug is the equilibrium state. If the interaction at the pore walls is strong, crystallization kinetics will slow due to immobilization effects. If the compartments are small and isolated, isothermal crystallization will require more time since each crystallizing subvolume must be homogeneously nucleated. Hence, different properties of the host system can be varied in order to efficiently suppress crystallization. The most important parameters that have to be optimised are pore size (d), pore topology and surface interactions (σ). By rationally adjusting these parameters, it should be possible to stabilize the amorphous state on a time scale relevant to potential applications for a broad class of drugs. Note that the solubility of amorphous pharmaceuticals is not significantly reduced in the nanoporous host systems used here since the large porosity and the bicontinuous morphology ensure high accessibility of the embedded drug for the solvent. First indicative experiments show that ACE confined to CPGs can be dissolved in water or ethanol at room temperature within a few minutes.

In summary, we have shown that nanoconfinement is a promising strategy to produce amorphous drugs which persist for long periods of time. It is demonstrated that amorphous ACE in untreated CPGs with a pore diameter $d = 4.6$ nm and hydroxyl-terminated pore walls is stable for weeks. Thermodynamic reasons as well as changes in the mobility and the nucleation behaviour might be the origin of this amorphization effect. The potential influences of pore diameter, pore topology and surface interactions were discussed. These parameters, which significantly affect the crystallization behaviour, should determine the performance of nanoporous host systems stabilizing the amorphous state of drugs in real-life applications.

Acknowledgements

Financial support by the state Sachsen-Anhalt in the framework of the research cluster "Nanostructured materials" is acknowledged.

Notes and references

1 (*a*) B. C. Hancock and G. Zografi, *J. Pharm. Sci.*, 1997, **86**, 1–12; (*b*) C. J. Roberts and P. G. DeBenedetti, *AIChE J.*, 2002, **48**, 1140–1144.
2 (*a*) B. C. Hancock and M. Parks, *Pharm. Res.*, 2000, **17**, 397–404; (*b*) D. Zhou, G. G. Z. Zhang, D. J. W. Grant and E. A. Schmitt, *J. Pharm. Sci.*, 2002, **91**, 1863–1872.
3 (*a*) R. Prasad and S. Lele, *Philos. Mag. Lett.*, 1994, **70**, 357–361; (*b*) C. L. Jackson and G. B. McKenna, *Chem. Mater.*, 1996, **8**, 2128–2137; (*c*) M. Alcoutlabi and G. B. McKenna, *J. Phys.: Condens. Matter*, 2005, **17**, R461–R524.
4 (*a*) D. Turnbull and R. L. Cormia, *J. Chem. Phys.*, 1961, **34**, 820–831; (*b*) Y. L. Loo, R. A. Register and A. J. Ryan, *Phys. Rev. Lett.*, 2000, **84**, 4120–4123; (*c*) G. Reiter, G. Castelein, J. U. Sommer, A. Röttele and T. Thurn-Albrecht, *Phys. Rev. Lett.*, 2001, **87**, 6101–6104; (*d*) M. V. Massa, J. L. Carvalho and K. Dalnoki-Veress, *Eur. Phys. J. E*, 2003, **12**, 111–117.
5 (*a*) M. Arndt, R. Stannarius, H. Groothues, E. Hempel and F. Kremer, *Phys. Rev. Lett.*, 1997, **79**, 2077–2080; (*b*) A. Schönhals, H. Göring, C. Schick, R. Zorn and B. Frick, *Colloid Polym. Sci.*, 2004, **282**, 882–891; (*c*) C. Alba-Simionesco, G. Doseeh, E. Dumont, B. Frick, B. Geil, D. Morineau, V. Teboul and Y. Xia, *Eur. Phys. J. E*, 2003, **12**, 19–28; (*d*) A. Schreiber, I. Ketelsen and G. H. Findenegg, *Phys. Chem. Chem. Phys.*, 2001, **3**, 1185–1195.
6 (*a*) A. Burger, *Acta Pharm. Technol.*, 1982, **28**, 1–20; (*b*) G. Nichols and C. S. Frampton, *J. Pharm. Sci.*, 1998, **87**, 684–693; (*c*) P. Espeau, R. Ceolin, J. L. Tamarit, M. A. Perrin, J. P. Gauchi and F. Leveiller, *J. Pharm. Sci.*, 2005, **94**, 524–539.
7 (*a*) M. Beiner, G. T. Rengarajan, S. Pankaj, D. Enke and M. Steinhart, *Nano Lett.*, 2007, **7**, 1381–1385; (*b*) G. T. Rengarajan and M. Beiner, *Lett. Drug Des. Discovery*, 2006, **3**, 723–730.
8 (*a*) G. P. Johari, S. Kim and R. M. Shanker, *J. Pharm. Sci.*, 2005, **54**, 2207–2223; (*b*) P. DiMartino, G. F. Palmeri and S. Martelli, *Chem. Pharm. Bull.*, 2000, **48**, 1105–1108.
9 This nominal rate corresponds to real quenching rates of at least −100 K min^{-1} when Perkin Elmer DSC7 and Pyris Diamond instruments are used.
10 (*a*) P. Di Martino, P. Conflant, M. Drache, J. P. Huvenne and A. M. Guyot-Hermann, *J. Therm. Anal.*, 1997, **48**, 447–458; (*b*) M. Szelagiewicz, C. Marcolli, S. Cianferani, A. P. Hard, A. Vit, A. Burkhard, M. von Raumer, U. C. Hofmeier, A. Zilian, E. Francotte and R. Schenker, *J. Therm. Anal. Calorim.*, 1999, **97**, 23–43; (*c*) M. L. Peterson, S. L. Morissette, C. McNulty, A. Goldsweig, P. Shaw, M. LeQuesne, J. Monagle, N. Encina, J. Marchionna, A. Johnson, J. Gonzalez-Zugasti, A. V. Lemmo, S. J. Ellis, M. J. Cima and O. Almarsson, *J. Am. Chem. Soc.*, 2002, **124**, 10958–10959.
11 (*a*) J. M. Ha, J. H. Wolf, M. A. Hillmyer and M. D. Ward, *J. Am. Chem. Soc.*, 2004, **126**, 3382–3383; (*b*) J. M. Ha, M. A. Hillmyer and M. D. Ward, *J. Chem. Phys.*, 2005, **109**, 1392–1399.
12 Note that the average volume of an acetaminophen molecule is about 0.2 nm^3 and that the unit cell of form III has a volume of about 0.77 nm^3 according to Peterson *et al.*[10c] The well known unit cells of form I and II reported by Nichols and Frampton[6b] have volumes of 0.75 nm^3 and 1.5 nm^3, respectively.